Mobile Robot Navigation Under Pose Uncertainty in Unknown Environments

Arvanitakis, I., Tzes, A. & Giannousakis, K.

DOI 10.1016/j.ifacol.2017.08.2267
ISSN 1474-6670

Publisher: International Federation of Automatic Control (IFAC)

Mobile Robot Navigation Under Pose Uncertainty in Unknown Environments ⋆

Ioannis Arvanitakis * **Anthony Tzes** ** **Konstantinos Giannousakis** *

* *Department of Electrical & Computer Engineering, University of Patras, Rio 26500, Achaia, Greece (e-mail: arvanitakis(giannousakis)@ece.upatras.gr).*
** *Engineering Division, New York University Abu Dhabi, Abu Dhabi, United Arab Emirates. (e-mail: anthony.tzes@nyu.edu).*

Abstract: Navigation of a mobile robot under uncertainty in pose information in an unknown environment is the subject of this paper. The mobile robot is equipped limited field of view limited-range finder and a magnetometer to infer its orientation. The target location is known, while the robot's localization suffers from measurement errors. The uncertainty is taken into consideration by calculation of the Guaranteed Visibility and Guaranteed Sensed Area, where safe navigation can be assumed regardless of the measurement error. A switching objective function initially guarantees the exploration towards the target area and afterwards safely guides the robot towards it. Simulation results that prove the efficiency of the proposed scheme are presented.

Keywords: Mobile robots, Pose sensing, Autonomous robotic systems, Guidance navigation and control, Intelligent robotics

1. INTRODUCTION

Autonomous navigation of mobile robots is an area of research with increasing interest over the years (**?**). Tasks such as area coverage (**??**), exploration, surveillance, search and rescue missions require that the robots move efficiently in the environment, avoiding obstacles during motion and keeping under consideration the robots' physical constraints.

Motion planning for known environments has been extensively researched over the past few decades (**?**), relying on principles such as the Artificial Potential Fields (**?**), the vector field histogram (**?**), probabilistic roadmaps (**?**) and Rapidly-exploring Random Trees (RRT) (**?**). Path planning methods such as the Dynamic Window Approach (**?**), that rely upon local real-time obstacle avoidance, have been implemented in uncertain or unknown environments (**?**) where the information about the environment in the vicinity of the robot is taken through onboard sensors. These methods, while effective, prove to be inefficient (**?**) in the aforementioned environments.

If the sensory information about the environment is utilized for an on-line map building process, then the sub-problem of exploration towards the unknown target area is included in the navigation. One of the first methods is the frontier based exploration (**?**), where a frontier is defined as the boundary between explored and unexplored space. The frontier concept has been widely used to research new exploration methods (**?**).

While recent sensors, such as LIDAR and vision based systems, provide accurate environment information measurements, localization techniques still suffer from noisy IMU-measurements. In the Simultaneous Localization and Mapping (SLAM) problem (**??**), the estimated pose contains a bounded error. This provides inaccurate maps, and the resulting navigation schemes that rely upon the created map may prove ineffective.

The problem imposed by the authors is the navigation of a mobile robot in an unknown environment with a known target location that needs to be discovered and under bounded pose uncertainty. A robot is equipped with a range sensor with a limited field of view and range, while localization information contains a bounded error. The contribution lays within the use of a switching objective function, where initially its optimization aims towards the exploration of the target. Uncertainty is taken into consideration by calculating both the Guaranteed Visibility and the Guaranteed Sensed Area, subspaces of the initial sensed and explored areas, where safe operation of the robot can be guaranteed in spite of these errors. Frontier exploration selection occurs via the minimization of a cost function. When the target position is discovered, the control law switches to a distance based navigation function to reach it.

The paper is structured as follows: in Section 2 some mathematical preliminaries are given and the problem formulation is presented, followed by Section 3 where the Guaranteed Visibility and Guaranteed Sensed Area are defined and calculated and the control law is given. In Section 4, simulation studies that outline the efficiency of the proposed method are presented, while in Section 5, conclusions are drawn.

2. PROBLEM FORMULATION

2.1 Mathematical Preliminaries

Consider a path-connected topological space $\mathcal{A} \subset \mathbb{R}^n$. The boundary of $\mathcal{A}$ is denoted as $\partial\mathcal{A}$, while $\{\mathcal{B}_i\}$, $i = 1, ..., N$

⋆ This work has received funding from the European Union Horizon 2020 Research and Innovation Programme under the Grant Agreement No. 644128, AEROWORKS.

denotes a collection of subsets. Spaces $\mathcal{A}, \mathcal{B}$ are considered disjoint if $\mathcal{A} \cap \mathcal{B} = \varnothing$.

The Minkowski sum of two spaces $\mathcal{A}, \mathcal{B}$ can be defined as the space given by $\mathcal{A} \oplus \mathcal{B} = \{a + b | a \in \mathcal{A}, b \in \mathcal{B}\}$.

Given the collection of all paths $\{\gamma_k\}$ that connect two arbitrary points $p_1, p_2 \in \mathcal{A}$, the length of the shortest path defines the geodesic metric $d_g(p_1, p_2)$ and the resulting path is called the geodesic path.

Definition 1. Let us consider $r \in \mathcal{A}$ and a subspace $\mathcal{B} \subseteq \mathcal{A}$. Then the geodesic Hausdorff distance is defined as the minimum geodesic distance of all points $q \in \mathcal{B}$ from r, i.e.

$$H_g(r, \mathcal{B}) = \min_{q \in \mathcal{B}} d_g(r, q) \; .$$

Definition 2. Consider a point $r \in \mathcal{A}$. The visibility subspace of $\mathcal{A}$ from r, shown in Fig. 1 is defined as a subset $\mathcal{A}^v(r; R)$, containing all points q, so that the geodesic path connecting r and q is a straight line and has length less than or equal to $R > 0$, i.e.

$$\mathcal{A}^v(r; R) = \{q \in \mathcal{A}; d_g(r, q) = \|r - q\| \leq R\} \; . \tag{1}$$

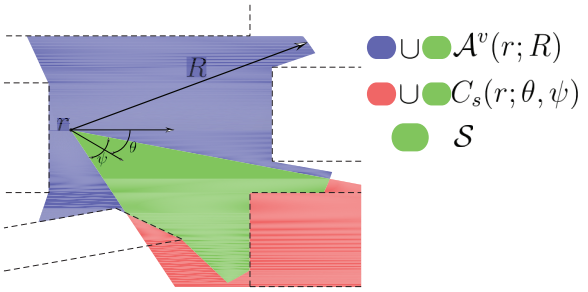

Fig. 1. Visibility subspace definition from an arbitrary position

Regarding notations, $\mathbb{I}_{n\times m}$ and $\mathbb{O}_{n\times m}$ denote the $n \times m$ identity and zero matrix respectively, while $L[\partial\mathcal{A}_k]$ denotes the length of the boundary segment $\partial\mathcal{A}_k$.

2.2 Problem Statement

Let a path connected space, $\Omega \subset \mathbb{R}^2$ be the unknown area of interest. Let $x = [\, r,\, \theta \,]^T = [\, (r_x,\, r_y),\, \theta \,]^T$ be the robot's state vector, where $r \in \Omega$ and $\theta \in \mathbb{R}$ be the position and orientation respectively, and $p_t \in \Omega$ be a goal position. The robot is equipped with a range sensor of circular sector pattern $C_s(r; \theta, \psi)$, with a sensing limit R and a field of view angle ψ, centered around its current heading, defined as the intersection of two semi-planes

$$C_s(r; \theta, \psi) \triangleq r + \left\{ \begin{bmatrix} -\tan^{-1}(\theta + \frac{\psi}{2}) & 1 \\ \tan^{-1}(\theta - \frac{\psi}{2}) & -1 \end{bmatrix} p \leq \begin{bmatrix} 0 \\ 0 \end{bmatrix} \right\} \; .$$

At any time instance, a sector visibility subspace

$$\mathcal{S} = \Omega^v(r; R) \cap C_s(r; \theta, \psi)$$

created by the range sensor is defined, while $\mathcal{A} \subseteq \Omega$ is the aggregated sensed area.

The following kinodynamic robot model is assumed

$$\begin{bmatrix} \dot{r} \\ \dot{\theta} \end{bmatrix} = \begin{bmatrix} u \\ \omega \end{bmatrix} \tag{2}$$

where $u \in \mathbb{R}^2, \omega \in \mathbb{R}$.

Under the assumption of noisy position and orientation measurements the robot's state vector $\tilde{x} = [\, \tilde{r},\, \tilde{\theta} \,]^T = [\, (\tilde{r}_x,\, \tilde{r}_y),\, \tilde{\theta} \,]^T$ is assumed to be within a set $\tilde{\mathcal{E}}$ defined as $\tilde{\mathcal{E}} = x \oplus \mathcal{E}$ where

$$\mathcal{E} = \{x \in \mathbb{R}^3 : [\, r_x \;\; r_y \,] \begin{bmatrix} r_x \\ r_y \end{bmatrix} \leq \varepsilon_d,\; |\theta| \leq \varepsilon_\theta\} \; , \tag{3}$$

A switching objective function is formulated (**?**), where subsets of spaces $\mathcal{S}$ $(\mathcal{A})$ - namely $\tilde{\mathcal{S}}$ $(\tilde{\mathcal{A}})$ must be found that take into account the uncertainty and ensure safe robot operation.

2.3 Guaranteed Visibility and Guaranteed Sensed Area

The imposed uncertainty affects the navigation by incorrect estimation on the created global map of the sensed area boundaries $\{\partial\mathcal{S}_l^o\} \subset \partial\Omega$. The aim is to define a new visibility subspace, called the Guaranteed Visibility $\tilde{\mathcal{S}} \subseteq \mathcal{S}$ - and consequently the Guaranteed Sensed Area derived from this subspace $\tilde{\mathcal{A}} \subseteq \mathcal{A}$ - where safe navigation for the robot can be ensured. Thus, initially given sensor measurements of the area boundary $\partial\mathcal{S}^o$, and localization uncertainty, the Boundary Uncertainty Space $\mathcal{C}$ must be defined.

All range sensor measurements can be well described in the local frame by a pair of polar coordinates (d_p, ψ_p), $d_p \in (0, R)$, $\psi_p \in [-\frac{\psi}{2}, \frac{\psi}{2}]$. The sensed cloud of points, expressed in a global frame, can be given by

$$p = \tilde{r} + \mathbf{R}(\tilde{\theta}) \begin{pmatrix} d_p \cos\psi_p \\ d_p \sin\psi_p \end{pmatrix} \; , \tag{4}$$

or, for brevity, $p = \tilde{r} + \mathbf{R}(\tilde{\theta})(d_p, \psi_p)$. $\mathbf{R}(\tilde{\theta})$ is the rotation matrix:

$$\mathbf{R}(\tilde{\theta}) = \begin{bmatrix} \cos\tilde{\theta} & -\sin\tilde{\theta} \\ \sin\tilde{\theta} & \cos\tilde{\theta} \end{bmatrix} \; .$$

Two additional spaces are introduced, namely $\tilde{\mathcal{E}}_r$ and $\tilde{\mathcal{E}}_\theta$ derived from projections of space $\tilde{\mathcal{E}}$.

$$\tilde{\mathcal{E}}_r = \left\{\tilde{r} \in \mathbb{R}^2 : \|\tilde{r} - r\| \leq \varepsilon_d\right\} \; ,$$
$$\tilde{\mathcal{E}}_\theta = \left\{\tilde{\theta} \in [\theta - \varepsilon_\theta, \theta + \varepsilon_\theta]\right\} \; .$$

The locus $\mathcal{C}_{\tilde{\theta}}$ of a sensor measurement (d_p, ψ_p) given orientation uncertainty can be given from:

$$\mathcal{C}_{\tilde{\theta}} = \left\{\tilde{r} + \mathbf{R}(\tilde{\theta})(d_p, \psi_p) \mid \tilde{\theta} \in \tilde{\mathcal{E}}_\theta\right\} \; . \tag{5}$$

Lastly, considering the additional position uncertainty creates locus $\mathcal{C}_{\tilde{r}}$ that can be calculated from:

$$\mathcal{C}_{\tilde{r}} = \mathcal{C}_{\tilde{\theta}} \oplus \tilde{\mathcal{E}}_r \; . \tag{6}$$

From (4) - (6) the Boundary Uncertainty Space $\mathcal{C}$ can be retrieved as

$$\mathcal{C}^o = \bigcup_{i=1}^{l} \partial\mathcal{S}_i^o \oplus \mathcal{C}_{\tilde{r}} \; ,$$
$$\mathcal{C} = \mathcal{C} \cup \mathcal{C}^o \; . \tag{7}$$

With the definition of $\mathcal{C}$, $\tilde{\mathcal{S}}$ can be derived as the sector visibility subspace of space $\mathcal{S} \setminus \mathcal{C}$, that is:

$$\tilde{\mathcal{S}} = (\mathcal{S} \setminus \mathcal{C})^{v} (\tilde{r}; R - \varepsilon_d) \cap C_s(r; \tilde{\theta}, \psi - 2\varepsilon_\theta) . \quad (8)$$

Where R and ψ are reduced to $R - \varepsilon_d$ and $\psi - 2\varepsilon_\theta$ to amend for the uncertainty. The Guaranteed Sensed Area, $\tilde{\mathcal{A}}$, can then be derived as

$$\tilde{\mathcal{A}} = \left(\tilde{\mathcal{A}} \cup \tilde{\mathcal{S}}\right) \setminus \mathcal{C} . \quad (9)$$

With the definition of $\tilde{\mathcal{S}}$ and $\tilde{\mathcal{A}}$ the objective function is formulated as

$$\mathcal{H}(\tilde{x}) = \int_{\tilde{\mathcal{S}}} f(p)\phi(p)dp \ , \ p_t \notin \tilde{\mathcal{S}} \quad (10)$$

during exploration phase and,

$$\mathcal{H}(\tilde{x}) = \frac{1}{\|p_t - \tilde{r}\|} \ , \ p_t \in \tilde{\mathcal{S}} \ , \quad (11)$$

during navigation to the goal position, where a) $f(p) : \tilde{\mathcal{A}} \to \mathbb{R}$ is the performance function and b) $\phi(p) : \tilde{\mathcal{A}} \to \mathbb{R}$ the weighting function.

3. PATH PLANNING UNDER UNCERTAINTY

3.1 Control Law Derivation

Theorem 3. Consider a robot with a sensing pattern of a circular sector with field of view angle ψ and range R, governed by its kinodynamics (2). The control law that optimizes the objective function (10) is given by

$$\begin{aligned}\begin{bmatrix} u \\ \omega \end{bmatrix} = &\sum_{i=1}^{k} \int_{\partial \mathcal{S}_i^c} f\phi \frac{\partial p}{\partial \tilde{x}}|_{p \in \partial \tilde{S}^c} n dp \ + \\ &\sum_{i=1}^{m} \int_{0}^{1} f_1\phi_1 \frac{\partial p}{\partial \tilde{x}}|_{p \in \partial \tilde{S}^\ell} \upsilon n d\upsilon \ + \\ &\sum_{i=1}^{2} \int_{0}^{1} f_2\phi_2 \frac{\partial p}{\partial \tilde{x}}|_{p \in \partial \tilde{S}^v} \upsilon n d\upsilon \ .\end{aligned} \quad (12)$$

where $f_1 = f(a_i + \upsilon(b_i - a_i))$, $\phi_1 = \phi(a_i + \upsilon(b_i - a_i))$, $i = 1, \ldots, m$, $f_2 = f(\tilde{r} + \upsilon(c_i - \tilde{r}))$, $\phi_2 = \phi(\tilde{r} + \upsilon(c_i - \tilde{r}))$, $i = 1, 2$ and

$$\frac{\partial p}{\partial \tilde{x}}|_{p \in \partial \tilde{S}^c} = \begin{bmatrix} 1 & 0 & -R\sin(\varphi + \tilde{\theta}) \\ 0 & 1 & R\cos(\varphi + \tilde{\theta}) \end{bmatrix} , \quad (13)$$

$$\frac{\partial p}{\partial \tilde{x}}|_{p \in \partial \tilde{S}^\ell} = \begin{bmatrix} -\dfrac{\|p_b - p_a\|}{\|\tilde{r} - p_a\|} \upsilon \mathbb{I}_{2\times 2} & \mathbb{O}_{2\times 1} \end{bmatrix} , \quad (14)$$

$$\frac{\partial p}{\partial \tilde{x}}|_{p \in \partial \tilde{S}^v} = \begin{bmatrix} 0 & 0 & -\upsilon\|\tilde{r} - c\|\sin(\varphi + \tilde{\theta}) \\ 0 & 0 & \upsilon\|\tilde{r} - c\|\cos(\varphi + \tilde{\theta}) \end{bmatrix} . \quad (15)$$

Proof. For the remainder of this proof, for notation simplicity, function variables of f and ϕ will be omitted. By differentiating (10) with respect to $\tilde{x} = [\tilde{r}\ \tilde{\theta}]^T$ and using the Leibniz integral rule we obtain

$$\frac{\partial \mathcal{H}}{\partial \tilde{x}} = \int_{\partial \mathcal{S}} f\phi \frac{\partial p}{\partial \tilde{x}}^T n dp \ , \quad (16)$$

where n is the outward unit normal vector to $\partial\tilde{\mathcal{S}}$.

Boundary $\partial\tilde{\mathcal{S}}$ can be decomposed into: a) a collection of l-segments that belong to visible boundary uncertainty space $\{\partial\tilde{\mathcal{S}}_l^o\} \subseteq \partial\mathcal{C}$, b) a collection of k-circular arcs $\{\partial\tilde{\mathcal{S}}_k^c\}$ created by the limit range of the sensor, c) a collection of m-line segments $\{\partial\mathcal{S}_m^\ell\}$ created by visibility constraints that may be denoted as $\{[a, b]_k\}$, $\|a - r\| < \|b - r\|$, and d) 2 line segments $\{\partial\tilde{\mathcal{S}}_{1,2}^v\}$ created by the limited field of view of the sensor, denoted as $\{[\tilde{r}, c]_k\}$.

Consequently, $\partial\tilde{\mathcal{S}}$ may be written as,

$$\partial\tilde{\mathcal{S}} = \bigcup_{i=1}^{l} \partial\tilde{\mathcal{S}}_i^o + \bigcup_{i=1}^{k} \partial\tilde{\mathcal{S}}_i^c + \bigcup_{i=1}^{m} \partial\tilde{\mathcal{S}}_i^\ell + \bigcup_{i=1}^{2} \partial\tilde{\mathcal{S}}_i^v \ . \quad (17)$$

Equation (16) is thus transformed to

$$\begin{aligned}\frac{\partial \mathcal{H}}{\partial \tilde{x}} = &\sum_{i=1}^{l} \int_{\partial\tilde{\mathcal{S}}_i^o} f\phi \frac{\partial p}{\partial \tilde{x}}^T n dp \ + \sum_{i=1}^{k} \int_{\partial\tilde{\mathcal{S}}_i^c} f\phi \frac{\partial p}{\partial \tilde{x}}^T n dp + \\ &\sum_{i=1}^{m} \int_{\partial\tilde{\mathcal{S}}_i^\ell} f\phi \frac{\partial p}{\partial \tilde{x}}^T n dp + \sum_{i=1}^{2} \int_{\partial\tilde{\mathcal{S}}_i^v} f\phi \frac{\partial p}{\partial \tilde{x}}^T n dp \ .\end{aligned} \quad (18)$$

Following this boundary analysis, the Jacobian $\partial p/\partial\tilde{x} = [\partial p/\partial\tilde{r} \ \ \partial p/\partial\tilde{\theta}]$ can be now calculated for each term of (18), by considering that we are dealing with a static boundary and computing the relative movement of an arbitrary point in the remaining free boundaries with respect to the robot position, which results in the Jacobians given from (13), (14) and (15).

As mentioned in subsection 2.2, this control input is applied to the robot until the target area is discovered, at which point the control law switches to a navigation function based on the shortest distance to target, $\|\tilde{r} - p_t\|$ and the gradient descent law constructs the final segment of the path.

3.2 Frontier Cost, Performance and Weighting Functions

Having calculated the control law, functions $f(p)$ and $\phi(p)$ should be appropriately selected taking into account the frontier based exploration process of the overall scheme.

Boundary $\partial\tilde{\mathcal{A}}$ is initially decomposed into two collections, part of the Boundary Uncertainty Space, $\{\partial\mathcal{A}_l^o\} \subseteq \mathcal{C}$ and free boundaries $\{\partial\mathcal{A}_k^f\}$. It should be noted that from the moment that $\tilde{\mathcal{A}}$ is partly the aggregated union over time of $\tilde{\mathcal{S}}$, a single free boundary $\partial\tilde{\mathcal{S}}_k^f$ can be any or a combination of the various boundaries mentioned in subsection 3.1. The various line segments (visibility constraints or field of view limits) are treated as possible frontiers, resulting the frontiers given by $\{\partial\mathcal{A}_k^f\}$.

Frontier selection should take into account the proximity of the frontier to the target, the proximity of the robot to the frontier and the accessibility to new unexplored areas. To implicate the proximity to target the introduction of the complimentary unexplored space $\mathcal{W}$, defined as

$$\mathcal{W} = \left[\mathbb{R}^2 \setminus \left(\tilde{\mathcal{A}} \cup \mathcal{C}\right)\right] \cup \tilde{\mathcal{A}} \, ,$$

that comprises from a collection of simply connected disjoint subsets. The frontier search is limited to frontiers that are boundaries of the disjoint subset $\mathcal{W}_d \subset \mathcal{W}$ that contains the target. The geodesic Hausdorff distance of a frontier from the target within $\mathcal{W}_d$ is then eligible to be used $H_g(p_t, \partial\tilde{\mathcal{A}}_k^f)$. Furthermore in space $\tilde{\mathcal{A}}$ the geodesic Hausdorff distance of the robot from a frontier $H_g(r, \partial\tilde{\mathcal{A}}_k^f)$ is calculated. Lastly, frontier length is taken into account in the cost function which takes the following form

$$\partial\tilde{\mathcal{A}}_c^f = \arg\min_j \Big(w_1 L \left[\partial\tilde{\mathcal{A}}_j^f\right]^{-1} + w_2 H_g(p_t, \partial\tilde{\mathcal{A}}_j^f) + w_3 H_g(r, \partial\tilde{\mathcal{A}}_j^f) \Big) \ , \quad (19)$$

where $w_i \in [0,1], i = 1,2,3$ are weights assigned to each part of the cost function.

Performance function $f(p)$ implicates the exploration process into the objective given by (10) and weighting function $\phi(p)$ implicates the navigation towards the desired position. The performance function will be defined as:

$$f(p) = \frac{1}{H_g(p, \tilde{\mathcal{A}}_c^f) + 1} \ . \quad (20)$$

This selection ensures that areas near the exploration frontier have greater importance. To give even greater importance in areas near the target, the weighting function $\phi(p)$ is defined as

$$\phi(p) = \frac{1}{d_g(y, p_t) + 1} \ , \quad (21)$$

$$y = \arg\min_{y \in \tilde{\mathcal{A}}_c^f} H_g(p_t, \tilde{\partial\mathcal{A}}_c^f) \ . \quad (22)$$

It must be noted that $d_g(y, p_t)$ refers to space $\mathcal{W}$.

4. SIMULATION STUDIES

The efficiency of the proposed scheme is verified through a simulation scenario. The area for navigation that was created is depicted in Fig. 2, where for visualization purposes the initial (green dot) and the target position (black dot) is illustrated.

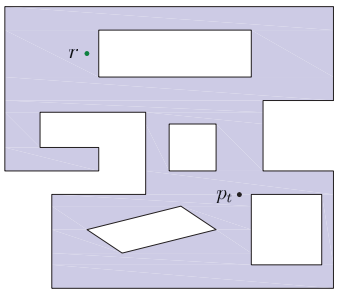

Fig. 2. Ω-sample area for navigation

The rectangle encapsulating the convex hull of Ω is of $14\,\mathrm{m} \times 12\,\mathrm{m}$. The robot has a range sensor of $R = 1.6\mathrm{m}$ and $\psi = 1.047\mathrm{rad}$, while the error space (3) has parameters $\varepsilon_d = 0.05\mathrm{m}$, $\varepsilon_\theta = 0.087\mathrm{rad}$. At each iteration step, the robot moves along the direction and towards the orientation given by equation (12) with a constant translational velocity of $\nu = 0.1\mathrm{m/sec}$ and angular velocity of $\omega = 0.1\mathrm{rad/sec}$. The weights of equation (19) are selected as $w_1 = 1, w_2 = 0.9$ and $w_3 = 0.4$. Boundaries of $\tilde{\mathcal{C}}$ and $\tilde{\mathcal{A}}$ at each step are archived using an OctoMap (**?**) like method with a grid resolution of $0.02\mathrm{m}$. In Fig. 3, the evolution of the navigation towards the target area is seen, where the 'light grey' area depicts the unknown space, the guaranteed sensed area corresponds to 'light blue' and the Boundary Uncertainty Space $\mathcal{C}$ is depicted from the 'dark grey' area. Boundaries of the Boundary Uncertainty Space $\partial\mathcal{C}$ are depicted with black, while with red the frontiers are depicted, and blue depicts the selected frontier given from equation (19). As may be seen in Figs. 3(a) - (b) given the limited field of view of the sensor and the orientation of the robot, it is able to move efficiently in exploring the selected frontier. As may be seen in Figs. 3(b) - (d), equation (19) is able to select the optimal frontier to explore and is capable of adapting to changes in the existing frontier. In Fig. 3(e) the switching to the shortest path towards target takes effect as the target is within the explored space. As seen in Fig. 3(f) the resulting path is sufficiently far from the Boundary Uncertainty Space to account for safe and fast navigation, without danger of collision, despite localization errors.

5. CONCLUSIONS

In this paper a novel method for navigation in unknown environments by a mobile robot with pose (position/orientation) uncertainty is presented. The robot is equipped with a ranged sensor with limited sensing range and field-of-view and position/orientation measurements contain a bounded error. Taking into account a target location in the unknown area and the sensed boundaries, the robot proceeds to find the Guaranteed Visibility $\tilde{\mathcal{S}}$ and Guaranteed Sensed Area $\tilde{\mathcal{A}}$, areas where safe navigation is ensured given the bounded localization error and the sensed boundaries of the area. Within it, it selects via minimization of a cost function a suitable frontier for exploration. A control law is implemented that moves the robot along the direction that maximizes an objective function that implicates the exploration towards the unknown area near the target. As soon as the target area is found, the motion control law switches over to the shortest length navigation function. Simulation results that prove the efficiency of the proposed scheme are presented.

REFERENCES

Arvanitakis, I., Giannousakis, K., and Tzes, A. (2016). Mobile robot navigation in unknown environment based on exploration principles. In *IEEE Conference on Control Applications (CCA)*, 493–498.

Bailey, T. and Durrant-Whyte, H. (2006). Simultaneous localization and mapping (slam): Part ii. *IEEE Robotics & Automation Magazine*, 13(3), 108–117.

Borenstein, J. and Koren, Y. (1991). The vector field histogram-fast obstacle avoidance for mobile robots. *IEEE Transactions on Robotics and Automation*, 7(3), 278–288.

Brock, O. and Khatib, O. (1999). High-speed navigation using the global dynamic window approach. In *IEEE International Conference on Robotics and Automation*, volume 1, 341–346 vol.1.

Durrant-Whyte, H. and Bailey, T. (2006). Simultaneous localization and mapping: part i. *IEEE robotics & automation magazine*, 13(2), 99–110.

Garcia, E., Jimenez, M., De Santos, P., and Armada, M. (2007). The evolution of robotics research. *Robotics Automation Magazine, IEEE*, 14(1), 90–103.

Haumann, A., Listmann, K., and Willert, V. (2010). Discoverage: A new paradigm for multi-robot exploration. In

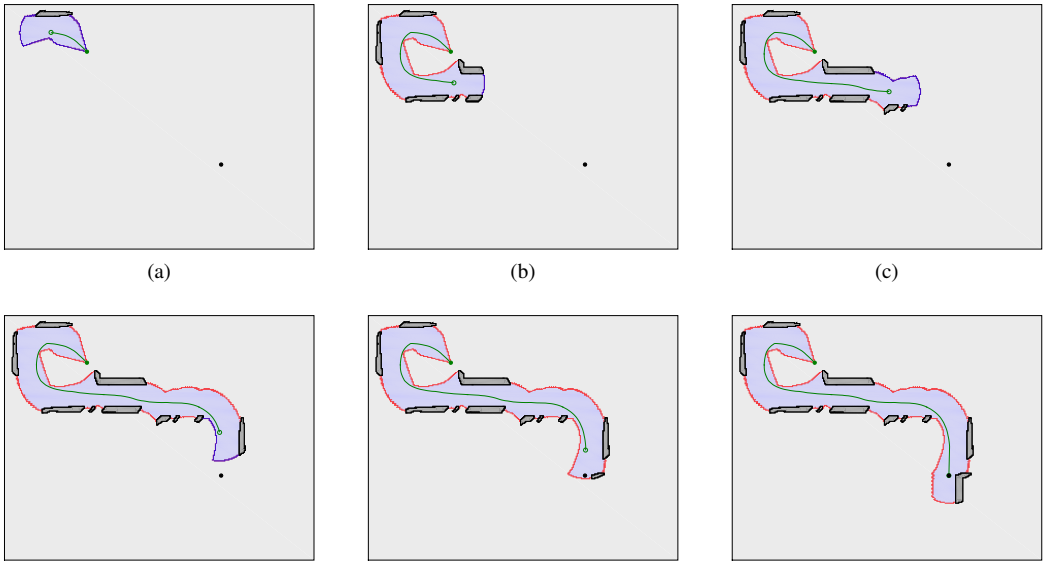

Fig. 3. Evolution of the robot navigation towards the target location

IEEE International Conference on Robotics and Automation (ICRA), 929–934.

Hornung, A., Wurm, K.M., Bennewitz, M., Stachniss, C., and Burgard, W. (2013). Octomap: an efficient probabilistic 3d mapping framework based on octrees. *Autonomous Robots*, 34(3), 189–206.

Kantaros, Y., Thanou, M., and Tzes, A. (2015). Distributed coverage control for concave areas by a heterogeneous robot-swarm with visibility sensing constraints. *Automatica*, 53, 195–207.

Kavraki, L., Svestka, P., Latombe, J.C., and Overmars, M. (1996). Probabilistic roadmaps for path planning in high-dimensional configuration spaces. *IEEE Transactions on Robotics and Automation*, 12(4), 566–580.

Khatib, O. (1986). Real-time obstacle avoidance for manipulators and mobile robots. *The International Journal of Robotics Research*, 5(1), 90–98.

Kuffner, J.J. and LaValle, S. (2000). Rrt-connect: An efficient approach to single-query path planning. In *IEEE International Conference on Robotics and Automation*, volume 2, 995–1001.

LaValle, S.M. (2006). *Planning Algorithms*. Cambridge University Press, Cambridge, U.K.

Stergiopoulos, Y. and Tzes, A. (2013). Spatially distributed area coverage optimisation in mobile robotic networks with arbitrary convex anisotropic patterns. *Automatica*, 49(1), 232–237.

Tovar, B., Murrieta-Cid, R., and LaValle, S. (2007). Distance-optimal navigation in an unknown environment without sensing distances. *IEEE Transactions on Robotics*, 23(3), 506–518.

Valero-Gomez, A., Gomez, J.V., Garrido, S., and Moreno, L. (2013). The path to efficiency: Fast marching method for safer, more efficient mobile robot trajectories. *IEEE Robotics Automation Magazine*, 20(4), 111–120.

Yamauchi, B. (1997). A frontier-based approach for autonomous exploration. In *IEEE International Symposium on Computational Intelligence in Robotics and Automation*, 146–151.